Inorg. Chem. **2003**, *42*, 7652–7657

Two Novel Vanadium Tellurites Covalently Bonded with Metal–Organic Complex Moieties: M(phen)V_2TeO_8 (M = Cu, Ni)

Dongrong Xiao,[†] Yangguang Li,[†] Enbo Wang,*[,†,‡] Shutao Wang,[†] Yu Hou,[†] Gejihu De,[†] and Changwen Hu[†]

Institute of Polyoxometalate Chemistry, Department of Chemistry, Northeast Normal University, Changchun, 130024, P. R. China, and State Key Laboratory of Structural Chemistry, Fujian Institute of Research on the Structure of Matter, Chinese Academy of Sciences, Fuzhou, 350002, People's Republic of China

Received March 13, 2003

Two novel two-dimensional organic–inorganic hybrid vanadium tellurites M(phen)V_2TeO_8 (M = Cu (**1**), Ni (**2**)) have been hydrothermally synthesized and characterized by the elemental analyses, IR spectra, EPR spectrum, XPS spectra, TG analyses, and single-crystal X-ray diffraction. Compound **1** crystallizes in the monoclinic system, space group $P2_1/c$, with $a = 9.2193(18)$ Å, $b = 7.9853(16)$ Å, $c = 21.401(4)$ Å, $\beta = 97.54(3)°$, and $Z = 4$. Compound **2** crystallizes in the monoclinic system, space group $P2_1/c$, with $a = 9.2163(18)$ Å, $b = 7.9897(16)$ Å, $c = 21.386(4)$ Å, $\beta = 97.52(3)°$, and $Z = 4$. Compounds **1** and **2** are isostructural, and both exhibit interesting two-dimensional networks with $[V_2TeO_8]_\infty$ double-chain-like ribbons bridged by metal–organic complex moieties $[M(phen)]^{2+}$ (M = Cu and Ni). Furthermore, the three-dimensional supramolecular architectures of compounds **1** and **2** are formed by π–π stacking interactions of phen groups between adjacent layers.

Organic−inorganic hybrid materials have been attracting extensive interest owing to their potential applications in catalysis, electron conductivity, magnetism, and photochemistry, as well as their intriguing structural features.[1−8] It is well-known that the functionality of organic−inorganic hybrid materials can be multiplied by the incorporation of organic and inorganic counterparts into one structural unit.[9−11] Recently, one remarkable feature in this field is that the organic components act as ligands directly coordinated to the inorganic scaffoldings or to the secondary metal centers.[12,13] On the basis of this mode, a large variety of organic−inorganic hybrid materials belonging to the $\{M_xL_y/V/O\}$, $\{M_xL_y/V/P/O\}$, $\{M_xL_y/Mo/O\}$, and $\{M_xL_y/Mo/P/O\}$ systems (M = transition metal, L = organic ligand) have been isolated,[12−18] which exhibit interesting one- (1-D), two- (2-D), and three-dimensional (3-D) structures. However, no study has ever been done in the $\{M_xL_y/V/Te/O\}$ system. In the past years, most efforts were concentrated on the preparation of pure inorganic vanadium tellurite phases, such as

* To whom correspondence should be addressed. E-mail: wangenbo@public.cc.jl.cn.
† Northeast Normal University.
‡ Fujian Institute of Research on the Structure of Matter.

(1) (a) Stupp, S. I.; Braun, P. V. *Science* **1997**, *277*, 1242−1248. (b) Kresge, C. T.; Leonowicz, M. E.; Roth, W. J.; Vartuli, J. C.; Beck, J. S. *Nature* **1992**, *359*, 710−712.
(2) Braun, P. V.; Osenar, P.; Tohver, V.; Kennedy, S. B.; Stupp, S. I. *J. Am. Chem. Soc.* **1999**, *121*, 7302−7309.
(3) Davis, M. E.; Lobo, R. E. *Chem. Mater.* **1992**, *4*, 756−768.
(4) Mialane, P.; Dolbecq, A.; Lisnard, L.; Mallard, A.; Marrot, J.; Sécheresse, F. *Angew. Chem., Int. Ed.* **2002**, *41*, 2398−2401.
(5) *Polyoxometalates*: *From Platonic Solids to Anti-Retroviral Activity*; Pope, M. T., Müller, A., Eds.; Kluwer Academic Publishers: Dordrecht, The Netherlands, 1994.
(6) Hill, C. L. *Chem. Rev.* **1998**, *98*, 1−2.
(7) Cheetham, A. K.; Férey, G.; Loiseau, T. *Angew. Chem., Int. Ed.* **1999**, *38*, 3268−3292.
(8) (a) Bu, X.-H.; Du, M.; Shang, Z.-L.; Zhang, R.-H.; Liao, D.-Z.; Shionoya, M.; Clifford, T. *Inorg. Chem.* **2000**, *39*, 4190−4199. (b) Bu, X.-H.; Liu, H.; Du, M.; Wong, K. M.-C.; Yam, V. W.-W.; Shionoya, M. *Inorg. Chem.* **2001**, *40*, 4143−4149. (c) Du, M.; Bu, X.-H.; Guo, Y.-M.; Liu, H.; Batten, S. R.; Ribas, J.; Mak, T. C. W. *Inorg. Chem.* **2002**, *41*, 4904−4908.
(9) Forster, P. M.; Cheetham, A. K. *Angew. Chem., Int. Ed.* **2002**, *41*, 457−459.
(10) Tao, J.; Zhang, X. M.; Tong, M. L.; Chen, X. M. *J. Chem. Soc., Dalton Trans.* **2001**, 770−771.
(11) Xu, L.; Lu, M.; Xu, B. B.; Wei, Y. G.; Peng, Z. H.; Powell, D. R. *Angew. Chem., Int. Ed.* **2002**, *41*, 4129−4132.
(12) (a) Hagrman, P. J.; Hagrman, D.; Zubieta, J. *Angew. Chem., Int. Ed.* **1999**, *38*, 2638−2684. (b) Hagrman, P. J.; Zubieta, J. *Inorg. Chem.* **2000**, *39*, 3252−3260. (c) LaDuuca, R. L., Jr.; Rarig, R. S., Jr.; Zubieta, J. *Inorg. Chem.* **2001**, *40*, 607−612. (d) Hagrman, P. J.; Zubieta, J. *Inorg. Chem.* **2001**, *40*, 2800−2809. (e) Hagrman, P. J.; Finn, R. C.; Zubieta, J. *Solid State Sci.* **2001**, *3*, 745−774.
(13) Liu, C.-M.; Hou, Y.-L.; Zhang, J.; Gao, S. *Inorg. Chem.* **2002**, *41*, 140−143.

10.1021/ic034272p CCC: $25.00
Published on Web 10/10/2003

$Te_2V_2O_9$,[19] α-$TeVO_4$,[20] β-$TeVO_4$,[21] $NaVTeO_5$,[22] $KVTeO_5$,[22] and $Cs(VO_2)_3(TeO_3)_2$,[23] but the vanadium tellurites templated by the organic molecules or covalently attached with metal−organic complex moieties have not been observed hitherto.

It is noteworthy that both vanadium and tellurium exhibit a variety of coordination geometry modes,[24−26] such as {VO_4} tetrahedron, {VO_6} octahedron, {VO_5} square pyramid, {TeO_3} trigonal pyramid, {TeO_4} folded square, and {TeO_5} square pyramid, which have led to a rich structural chemistry of vanadium tellurites. Thus, it can be presumed that the introduction of metal−organic complex moieties into the vanadium tellurite phases may further enrich the structural motif of V−Te−O frameworks, which has been proved an effective way in the preparation of {V/O} and {V/P/O} systems. Furthermore, it is noteworthy that vanadium tellurite glasses exhibit large third-order nonlinear susceptibility, high infrared transmittance, and semiconducting property, showing special applications in semiconductive and optical materials.[27−32] Therefore, the preparation of novel vanadium tellurites has an intriguing perspective.

In this paper, we report the hydrothermal synthesis and crystal structure of two novel vanadium tellurites, Cu(phen)-V_2TeO_8 (**1**) and Ni(phen)V_2TeO_8 (**2**), which represent the first vanadium tellurites covalently bonded with the metal−organic complex moieties.

Experimental Section

General Considerations. All chemicals were commercially purchased and used without further purification. Elemental analyses (C, H, and N) were performed on a Perkin-Elmer 2400 CHN elemental analyzer. Cu, Ni, V, and Te were determined by a PLASMA-SPEC(I) ICP atomic emission spectrometer. EPR spectrum was recorded on a Japanese JES-FE3AX spectrometer at 293 K. XPS analyses were performed on a VG ESCALABMKII spectrometer with an Mg Kα (1253.6 ev) achromatic X-ray source. The vacuum inside the analysis chamber was maintained at 6.2×10^{-6} Pa during the analysis. IR spectra were recorded in the range 400−4000 cm^{-1} on an Alpha Centaurt FT/IR spectrophotometer using KBr pellets. TG analyses were performed on a Perkin-Elmer TGA7 instrument in flowing N_2 with a heating rate of 10 °C min^{-1}.

Synthesis of M(phen)V_2TeO_8 (M = Cu and Ni). Compound **1** was hydrothermally synthesized under autogenous pressure. A mixture of $CuCl_2 \cdot 2H_2O$ (0.25 mmol), V_2O_5 (0.5 mmol), Na_2TeO_3 (1 mmol), phen (0.5 mmol), and H_2O (9 mL) was stirred for 30 min in air. The mixture was then sealed in a 18 mL Teflon-lined autoclave, which was heated to 170 °C for 144 h. After slow cooling to room temperature, the resulting green needle crystals **1** were filtered off, washed with distilled water, and dried at ambient temperature (yield: 43% based on V). The green crystals were manually selected for structural determination and further characterization. Anal. Calcd for $C_{12}H_8N_2O_8CuTeV_2$ (**1**): C, 24.0; H, 1.3; N, 4.7; Cu, 10.6; Te, 21.2; V, 17.0. Found: C, 23.8; H, 1.2; N, 4.5; Cu, 10.7; Te, 21.1; V, 17.1. FT/IR data (cm^{-1}) for **1**: 3051 (m), 1606 (m), 1584 (m), 1515 (s), 1493 (w), 1423 (s), 1342 (w), 1228 (m), 1200 (w), 1140 (s), 1108 (m), 1049 (w), 977 (w), 967 (s), 939 (s), 872 (s), 851 (m), 780 (s), 720 (s), 651 (s), 504 (w), 462 (w), 433 (w).

The preparation of **2** was similar to that of **1** except that $NiCl_2 \cdot 6H_2O$ was used in place of $CuCl_2 \cdot 2H_2O$ (yield: 31% based on V). Anal. Calcd for $C_{12}H_8N_2O_8NiTeV_2$ (**2**): C, 24.2; H, 1.4; N, 4.7; Ni, 9.8; Te, 21.4; V, 17.1. Found: C, 24.0; H, 1.3; N, 4.5; Ni, 9.9; Te, 21.3; V, 17.2. FT/IR data (cm^{-1}) for **2**: 3443 (bh), 3053 (m), 1585 (m), 1516 (s), 1494 (w), 1425 (s), 1384 (w), 1343 (w), 1228 (m), 1141 (m), 1108 (m), 967 (s), 939 (s), 872 (s), 851 (s), 780 (s), 721 (s), 654 (s), 463 (w), 434 (w).

X-ray Crystallography. A green single crystal of **1** with dimensions of 0.378 × 0.114 × 0.113 mm was mounted inside a glass fiber capillary. The data were collected on a Rigaku R-AXIS RAPID IP diffractometer with Mo Kα ($\lambda = 0.710\ 73$ Å) at 293 K in the range of $1.92 < \theta < 27.34°$. An empirical absorption correction was applied. A total of 5746 (3494 unique, $R_{int} = 0.0282$) reflections were measured ($-11 \le h \le 11$, $-10 \le k \le 10$, $-27 \le l \le 27$).

A green single crystal of **2** with dimensions of 0.678 × 0.101 × 0.095 mm was mounted inside a glass fiber capillary. The data were collected on a Rigaku R-AXIS RAPID IP diffractometer with Mo Kα ($\lambda = 0.710\ 73$ Å) at 293 K in the range of $1.92 < \theta < 27.48°$. An empirical absorption correction was applied. A total of

(14) (a) You, W. S.; Wang, E. B.; Xu, Y.; Li, Y. G.; Xu, L.; Hu, C. W. *Inorg. Chem.* **2001**, *40*, 5468−5471. (b) Bi, L. H.; Wang, E. B.; Peng, J.; Huang, R. D.; Xu, L.; Hu, C. W. *Inorg. Chem.* **2000**, *39*, 671−679. (c) Li, Y. G.; Wang, E. B.; Zhang, H.; Luan, G. Y.; Hu, C. W. *J. Solid State Chem.* **2002**, *163*, 10−16. (d) Xu, L.; Sun, Y.; Wang, E.; Shen, E.; Liu, Z.; Hu, C.; Xing, Y.; Lin, Y.; Jia, H. *New J. Chem.* **1999**, *23*, 1041−1044. (e) Yuan, M.; Li, Y. G.; Wang, E. B.; Lu, Y.; Hu, C. W.; Hu, N. H.; Jia, H. Q. *J. Chem. Soc., Dalton Trans.* **2002**, 2916−2920. (f) Lu, Y.; Wang, E. B.; Yuan, M.; Luan, G. Y.; Li, Y. G. *J. Chem. Soc., Dalton Trans.* **2002**, 3029−3031. (g) Luan, G. Y.; Li, Y. G.; Wang, S. T.; Wang, E. B.; Han, Z. B.; Hu, C. W.; Hu, N. H.; Jia, H. Q. *J. Chem. Soc., Dalton Trans.* **2003**, 233−235. (h) Li, Y. G.; De, G. J. H.; Yuan, M.; Wang, E. B.; Huang, R. D.; Hu, C. W.; Hu, N. H.; Jia, H. Q. *J. Chem. Soc., Dalton Trans.* **2003**, 331−334. (i) Chen, Y. M.; Wang, E. B.; Lin, B. Z.; Wang, S. T. *J. Chem. Soc., Dalton Trans.* **2003**, 519−520. (j) Hu, C. W.; He, Q. L.; Zhang, Y. H.; Liu, Y. Y.; Zhang, Y. F.; Tang, T. D.; Zhang, J. Y.; Wang, E. B. *Chem. Commun.* **1996**, 121−122.

(15) (a) Zhang, X. M.; Tong, M. L.; Feng, S. H.; Chen, X. M. *J. Chem. Soc., Dalton Trans.* **2001**, 2069−2070. (b) Zhang, X. M.; Tong, M. L.; Chen, X. M. *Chem. Commun.* **2000**, 1817−1818.

(16) (a) Liu, C.-M.; Gao, S.; Hu, H.-M.; Wang, Z.-M. *Chem. Commun.* **2001**, 1636−1637. (b) Liu, C.-M.; Gao, S.; Kou, H.-Z. *Chem. Commun.* **2001**, 1670−1671.

(17) (a) Zhang, L. R.; Shi, Z.; Yang, G. Y.; Chen, X. M.; Feng, S. H. *J. Chem. Soc., Dalton Trans.* **2000**, 275−278. (b) Shi, Z.; Feng, S. H.; Gao, S.; Zhang, L.; Yang, G.; Hua, J. *Angew. Chem., Int. Ed.* **2000**, *39*, 2325−2327.

(18) (a) Huang, L.-H.; Kao, H.-M.; Lii, K.-H. *Inorg. Chem.* **2002**, *41*, 2936−2940. (b) Zheng, L.-M.; Zhao, J.-S.; Lii, K.-H.; Zhang, L.-Y.; Liu, Y.; Xin, X.-Q. *J. Chem. Soc., Dalton Trans.* **1999**, 939−944.

(19) Darriet, J.; Galy, J. *Cryst. Struct. Commun.* **1973**, *2*, 237−238.

(20) Meunier, G.; Darriet, J.; Galy, J. *J. Solid State Chem.* **1972**, *5*, 314−320.

(21) Meunier, G.; Darriet, J.; Galy, J. *J. Solid State Chem.* **1973**, *6*, 67−73.

(22) Darriet, J.; Guillaume, G.; Wilhelmi, K.-A.; Galy, J. *Acta Chem. Scand.* **1972**, *26*, 59−70.

(23) Harrison, W. T. A.; Buttery, J. H. N. *Z. Anorg. Allg. Chem.* **2000**, *626*, 867−870.

(24) Balraj, V.; Vidyasagar, K. *Inorg. Chem.* **1998**, *37*, 4764−4774.

(25) Balraj, V.; Vidyasagar, K. *Inorg. Chem.* **1999**, *38*, 1394−1400.

(26) Balraj, V.; Vidyasagar, K. *Inorg. Chem.* **1999**, *38*, 3458−3462.

(27) Nasu, H.; Matsushita, O.; Kamiya, K.; Kobayashi, H.; Kubodera, K. *J. Non-Cryst. Solids* **1990**, *124*, 275−277.

(28) Kim, S.; Yoko, H. T.; Sakka, S. *J. Am. Cream. Soc.* **1993**, *76*, 2486.

(29) Burger, H.; Vogel, W.; Kozhukharov, V. *Infrared Phys.* **1985**, *25*, 395−409.

(30) Rhee, C.; Yoon, S. W.; Lim, H. J. *Proc. 10th Int. Congr. Glass Kyoto, Jpn.* **1974**, *7*, 51.

(31) Rossognol, J.; Reau, M.; Tanguy, B.; Videau, J.; Porrtier, J. *J. Non-Cryst. Solids* **1993**, *162*, 244−252.

(32) Tanabe, S.; Hirao, K.; Soga, N. *J. Non-Cryst. Solids* **1990**, *122*, 79−82.

Table 1. Crystal Data and Structure Refinement for **1** and **2**

param	**1**	**2**
chem formula	$C_{12}H_8N_2CuO_8TeV_2$	$C_{12}H_8N_2NiO_8TeV_2$
fw	601.22	596.39
T (K)	293(2)	293(2)
λ (Å)	0.710 73	0.710 73
space group	$P2_1/c$	$P2_1/c$
a (Å)	9.2193(18)	9.2163(18)
b (Å)	7.9853(16)	7.9897(16)
c (Å)	21.401(4)	21.386(4)
β (deg)	97.54(3)	97.52(3)
V (Å^3)	1561.9(5)	1561.3(5)
Z	4	4
D_c (g/cm^3)	2.557	2.537
μ (mm^{-1})	4.400	4.246
R1[a]	0.0270	0.0218,
wR2[b]	0.0670	0.0611

[a] $R1 = \sum||F_o| - |F_c||/\sum|F_o|$. [b] $wR_2 = \sum[w(F_o^2 - F_c^2)^2]/\sum[w(F_o^2)^2]^{1/2}$.

Table 2. Selected Bond Lengths (Å) and Angles (deg) for **1**[a]

Te−O(8)	1.847(3)	Te−O(2)$^{\#1}$	1.980(3)
Te−O(1)	1.900(3)	Te−O(7)$^{\#2}$	2.399(3)
V(1)−O(3)	1.601(4)	V(1)−O(4)$^{\#3}$	1.787(3)
V(1)−O(7)	1.666(3)	V(1)−O(1)	1.815(3)
V(2)−O(6)	1.630(3)	V(2)−O(4)	1.768(3)
V(2)−O(5)	1.693(3)	V(2)−O(2)	1.778(3)
Cu−N(1)	2.013(3)	Cu−N(2)	1.993(3)
Cu−O(8)	1.927(3)	Cu−O(5)	1.937(3)
Cu−O(6)$^{\#1}$	2.271(3)		

O(8)−Te−O(1)	94.89(13)	O(8)−Te−O(7)$^{\#2}$	84.75(12)
O(8)−Te−O(2)$^{\#1}$	94.66(13)	O(1)−Te−O(7)$^{\#2}$	82.99(13)
O(1)−Te−O(2)$^{\#1}$	89.27(14)	O(2)$^{\#1}$−Te−O(7)$^{\#2}$	172.16(12)
O(8)−Cu−O(5)	88.35(12)	N(2)−Cu−N(1)	82.55(14)
O(8)−Cu−N(2)	90.74(13)	O(8)−Cu−O(6)$^{\#1}$	96.63(12)
O(5)−Cu−N(2)	171.50(14)	O(5)−Cu−O(6)$^{\#1}$	93.66(12)
O(8)−Cu−N(1)	169.02(13)	N(2)−Cu−O(6)$^{\#1}$	94.84(13)
O(5)−Cu−N(1)	97.00(14)	N(1)−Cu−O(6)$^{\#1}$	92.62(13)
O(6)−V(2)−O(5)	107.37(16)	O(6)−V(2)−O(2)	110.70(15)
O(6)−V(2)−O(4)	110.23(16)	O(5)−V(2)−O(2)	109.07(15)
O(5)−V(2)−O(4)	109.42(17)	O(4)−V(2)−O(2)	110.00(17)
O(3)−V(1)−O(7)	108.69(18)	O(3)−V(1)−O(1)	110.41(18)
O(3)−V(1)−O(4)$^{\#3}$	112.22(18)	O(7)−V(1)−O(1)	109.69(16)
O(7)−V(1)−O(4)$^{\#3}$	107.20(17)	O(4)$^{\#3}$−V(1)−O(1)	108.56(15)
Te−O(8)−Cu	113.45(14)	V(2)−O(6)−Cu$^{\#5}$	118.84(16)
V(2)−O(5)−Cu	154.3(2)	V(2)−O(2)−Te$^{\#5}$	132.31(16)
V(1)−O(1)−Te	131.63(18)	V(1)−O(7)−Te$^{\#6}$	121.44(17)
V(2)−O(4)−V(1)$^{\#4}$	153.4(2)		

[a] Symmetry transformations used to generate equivalent atoms: #1, $-x + 1, y - 1/2, -z + 1/2$; #2, $-x, y + 1/2, -z + 1/2$; #3, $x - 1, y, z$; #4, $x + 1, y, z$; #5, $-x + 1, y + 1/2, -z + 1/2$; #6, $-x, y - 1/2, -z + 1/2$.

6320 (3578 unique, $R_{int} = 0.0196$) reflections were measured ($-11 \le h \le 11$, $-9 \le k \le 10$, $-27 \le l \le 27$).

The structures of **1** and **2** were solved by the direct method and refined by full-matrix least squares on F^2 using the SHELXTL-97 software.[33] All of the non-hydrogen atoms were refined anisotropically. The hydrogen atoms were located from the Fourier difference maps. A summary of crystal data and structure refinement for compounds **1** and **2** is provided in Table 1. Selected bond lengths and angles of **1** and **2** are listed in Tables 2 and 3, respectively.

CCDC reference nos.: 200436 for **1**; 200435 for **2**.

Results and Discussion

Crystal Structures of 1 and 2. The single-crystal X-ray diffraction analysis reveals that compounds **1** and **2** are isostructural and both consist of a novel double-chain-like vanadium tellurite ribbon bridged by metal−phen complex moieties. The asymmetric units of **1** (Figure 1) and **2** (Figure S1) both exhibit two crystallographically independent V centers. The V(1) site shows a distorted tetrahedral coordination geometry with a terminal oxygen and three bridging oxygen atoms, two of which are linked with two Te centers and another one linked with V(2). The V(2) center shows a tetrahedral environment sharing two oxygen atoms with a

Table 3. Selected Bond Lengths (Å) and Angles (deg) for **2**[a]

Te−O(8)	1.837(2)	Te−O(2)$^{\#1}$	1.987(2)
Te−O(1)	1.903(2)	Te−O(7)$^{\#2}$	2.394(3)
V(1)−O(3)	1.603(3)	V(1)−O(4)$^{\#3}$	1.791(3)
V(1)−O(7)	1.671(2)	V(1)−O(1)	1.807(2)
V(2)−O(6)	1.626(2)	V(2)−O(4)	1.763(3)
V(2)−O(5)	1.691(2)	V(2)−O(2)	1.772(2)
Ni−O(8)	1.925(2)	Ni−N(2)	1.995(3)
Ni−O(5)	1.942(2)	Ni−N(1)	2.011(3)
Ni−O(6)$^{\#1}$	2.268(2)		

O(8)−Te−O(1)	95.17(10)	O(8)−Te−O(7)$^{\#2}$	84.85(9)
O(8)−Te−O(2)$^{\#1}$	94.56(10)	O(1)−Te−O(7)$^{\#2}$	82.92(10)
O(1)−Te−O(2)$^{\#1}$	89.44(11)	O(2)$^{\#1}$−Te−O(7)$^{\#2}$	172.24(9)
O(8)−Ni−O(5)	87.99(9)	N(2)−Ni−N(1)	82.54(11)
O(8)−Ni−N(2)	90.93(10)	O(8)−Ni−O(6)$^{\#1}$	96.57(9)
O(5)−Ni−N(2)	171.41(10)	O(5)−Ni−O(6)$^{\#1}$	93.71(9)
O(8)−Ni−N(1)	169.19(10)	N(2)−Ni−O(6)$^{\#1}$	94.88(10)
O(5)−Ni−N(1)	97.18(10)	N(1)−Ni−O(6)$^{\#1}$	92.58(9)
O(3)−V(1)−O(7)	108.69(14)	O(3)−V(1)−O(1)	110.27(14)
O(3)−V(1)−O(4)$^{\#3}$	112.39(14)	O(7)−V(1)−O(1)	109.46(12)
O(7)−V(1)−O(4)$^{\#3}$	107.26(13)	O(4)$^{\#3}$−V(1)−O(1)	108.69(12)
O(6)−V(2)−O(5)	107.31(12)	O(6)−V(2)−O(2)	110.43(12)
O(6)−V(2)−O(4)	110.31(13)	O(5)−V(2)−O(2)	108.85(11)
O(5)−V(2)−O(4)	109.66(13)	O(4)−V(2)−O(2)	110.23(13)
V(1)−O(1)−Te	131.82(14)	V(2)−O(5)−Ni	153.96(15)
V(2)−O(2)−Te$^{\#4}$	132.34(12)	V(2)−O(6)−Ni$^{\#4}$	119.09(12)
V(2)−O(4)−V(1)$^{\#5}$	153.49(18)	V(1)−O(7)−Te$^{\#6}$	121.62(12)
Te−O(8)−Ni	113.81(11)		

[a] Symmetry transformations used to generate equivalent atoms: #1, $-x + 1, y - 1/2, -z + 1/2$; #2, $-x, y + 1/2, -z + 1/2$; #3, $x - 1, y, z$; #4, $-x + 1, y + 1/2, -z + 1/2$; #5, $x + 1, y, z$; #6, $-x, y - 1/2, -z + 1/2$.

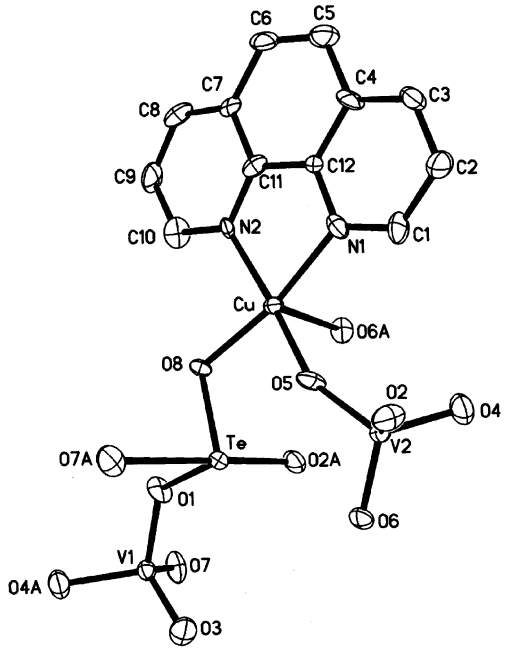

Figure 1. ORTEP drawing of compound **1** with thermal ellipsoids at 50% probability. H atoms are omitted for clarity.

(33) (a) Sheldrick, G. M. *SHELXS 97, Program for Crystal Structure Solution*; University of Göttingen: Göttingen, Germany, 1997. (b) Sheldrick, G. M. *SHELXL 97, Program for Crystal Structure Refinement*; University of Göttingen: Göttingen, Germany, 1997.

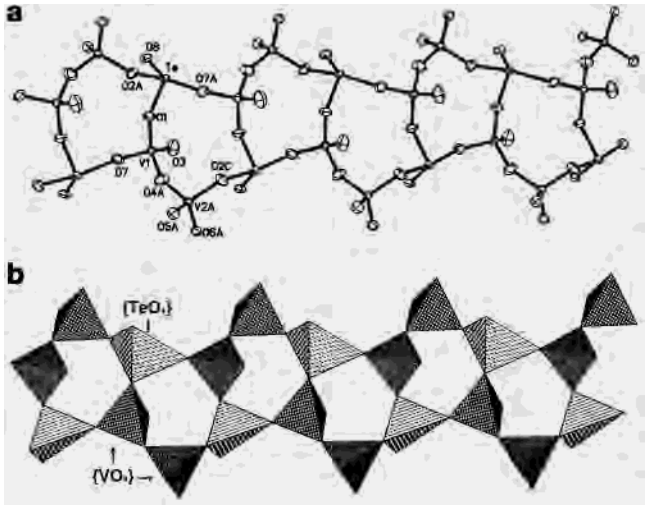

Figure 2. (a) Double-chain-like ribbon of $\{V_2TeO_8\}_\infty$ in **1**. (b) Polyhedral representative of the double-chain-like ribbon.

Cu or Ni atom, one oxygen atom with the V(1) site and the other one with Te atom. The V−O bond lengths are in the range of 1.601(4)−1.815(3) Å, and the O−V−O angles vary from 107.20(17) to 112.39(14)°. The Cu or Ni center adopts a square pyramidal geometry,[37,38] being coordinated by two nitrogen donors of a phen group, two oxygen atoms of the $\{V(2)O_4\}$ unit, and one oxygen atom of the $\{TeO_4\}$ unit. In the $\{TeO_4\}$ unit, three oxygen atoms bridge to two V(1) atoms and one V(2) atom and the fourth oxygen atom is linked with a Cu or Ni atom. The geometry of $\{TeO_4\}$ can be explained by VSEPR theory as an AX_4E trigonal bipyramid, in which the lone pair electrons occupy one equatorial position.[34,35] The Te−O bond lengths vary from 1.837(2) to 2.399(3) Å, and the two axial bonds are longer than the two equatorial ones. The O−Te−O angles are in the range of 82.92(10)−172.24(9)°.

The structures of **1** and **2** consist of novel infinite double-chain-like vanadium tellurite ribbons along the *b* axis, as shown in Figure 2a. In the double-chain-like ribbon, the $\{V(1)O_4\}$ tetrahedra, $\{TeO_4\}$ folded squares, and $\{V(2)O_4\}$ tetrahedra connect with each other in the corner-sharing mode and form a spiral-shaped chain. Two adjacent chains are connected together via the V(1)−O−Te bonds, forming the double-chain-like ribbon (Figure 2b). The ribbon consists of five-membered rings $\{V_3Te_2O_5\}$. The most interesting structural feature is that the adjacent $\{V_2TeO_8\}_\infty$ ribbons are covalently connected together by the $[M(phen)]^{2+}$ (M = Cu, Ni) complex moieties to form an interesting 2-D network (Figure 3). To our knowledge, such vanadium tellurites decorated by metal−organic complex moieties have never been reported. In the 2-D network, three-membered rings $\{MVTeO_3\}$ (M = Cu, Ni) and six-membered rings

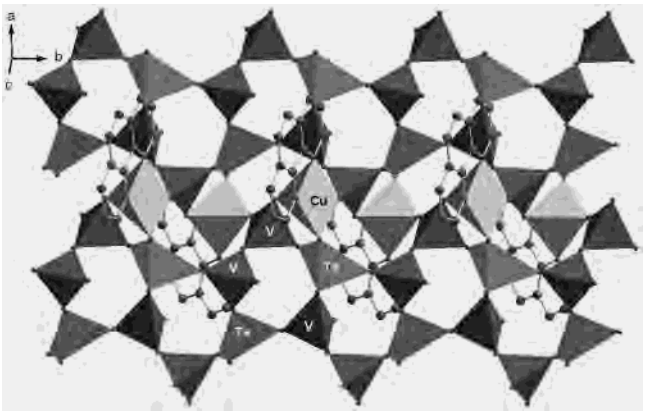

Figure 3. View of the organic−inorganic 2-D network of **1**.

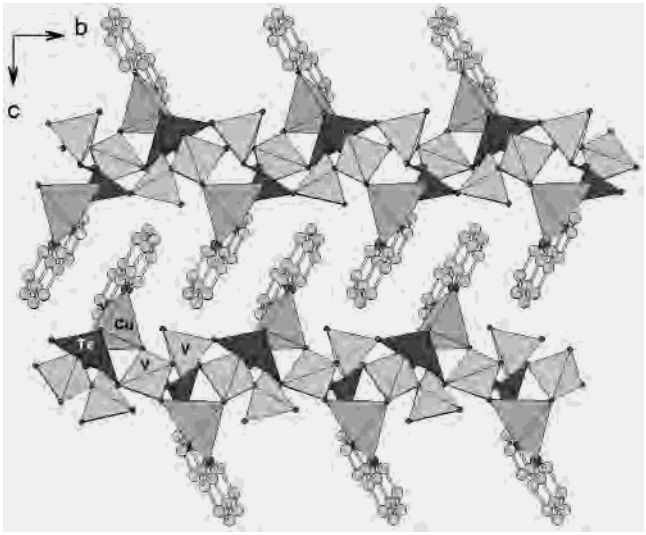

Figure 4. Packing arrangement of compound **1**, viewed along the *a* axis direction.

$\{M_2V_3TeO_6\}$ (M = Cu, Ni) are formed between adjacent double-chain ribbons. Thus, the novel organic−inorganic hybrid layer may be viewed as a network with a 3,5,6-net. The phen groups project above and below the 2-D network.

In the packing arrangement (see Figure 4 and Figure S3) of **1** and **2**, the adjacent layers are stably packed together via the $\pi-\pi$ stacking interactions of the phen groups. The close contact distance between the adjacent phen rings is 3.445 Å in **1** and 3.454 Å in **2**. Therefore, an interesting 3-D supramolecular architecture is formed.

The bond valence sum calculations[36] indicate that all V sites are in the +5 oxidation state and the Te site is in the +4 oxidation state in both **1** and **2**. The bond valence analysis also shows that both Cu and Ni sites are in the +2 oxidation state. The EPR spectrum and XPS spectra of compound **1** and **2** further confirm the above calculated results. The EPR (see Figure 5) spectrum of **1** at room temperature shows a Cu^{2+} signal with $g = 2.115$,[44] in accordance with the bond

(34) Johnston, M. G.; Harrison, W. T. A. *J. Am. Chem. Soc.* **2002**, *124*, 4576−4577.
(35) Gillsepie, R. J. *Molecular Geometry*; Van Norstand-Reinholdt: London, 1972.
(36) Brown, D.; Altermatt, D. *Acta Crystallogr.* **1985**, *B41*, 244−247.
(37) Raymond, K. N.; Corfield P. W. R.; Ibers, J. A. *Inorg. Chem.* **1968**, *7*, 1362−1372.
(38) Spiro, T. G.; Terzis A.; Raymond, K. N. *Inorg. Chem.* **1970**, *9*, 2415−2420.
(39) Nefedov, V. I.; Firsov, M. N.; Shaplygin, I. S. *J. Electron Spectrosc. Relat. Phenom.* **1982**, *26*, 65−78.
(40) (a) Larsson, R.; Folkesson, B.; Schön, G. *Chem. Scr.* **1973**, *3*, 88−90. (b) Kasperkiewicz, J.; Kovacich, J. A.; Lichtman, D. *J. Electron Spectrosc. Relat. Phenom.* **1983**, *32*, 128−132.
(41) Garbassi, F.; Bart. J. C. J.; Petrini, G. *J. Electron Spectrosc. Relat. Phenom.* **1981**, *22*, 95−107.

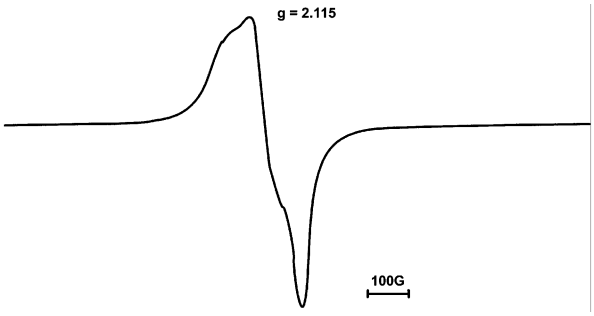

Figure 5. EPR spectrum of compound **1** showing a Cu^{2+} signal with $g = 2.115$.

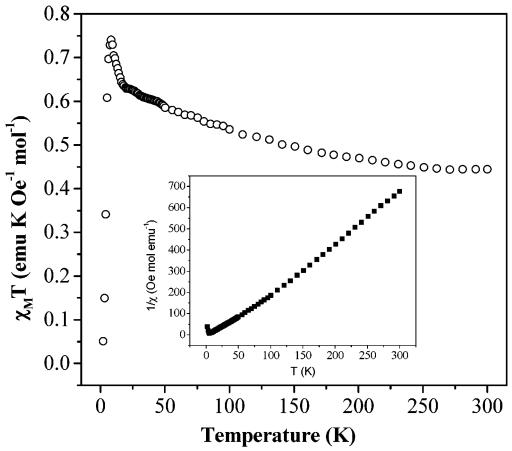

Figure 6. Plot of $\chi_M T$ vs temperature for **1**. The inset shows the inverse susceptibility with a linear regression based on upon the Curie−Weiss law.

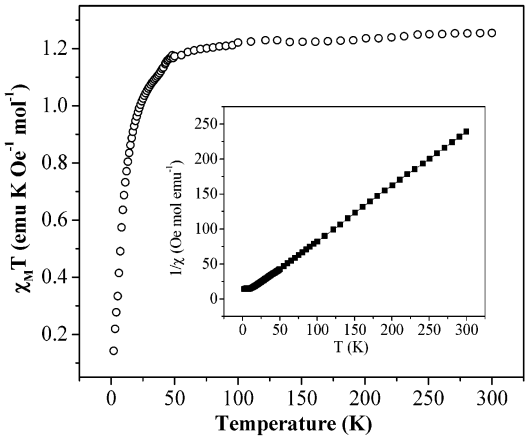

Figure 7. Plot of $\chi_M T$ vs temperature for **2**. The inset shows the inverse susceptibility with a linear regression based on upon the Curie−Weiss law.

valence sum calculations. The XPS spectra of compound **1** in the energy regions of Cu_{2p}, V_{2p}, and Te_{3d} show peaks at 934.0, 516.7, and 576.1 eV, attributable to Cu^{2+},[39,43] V^{5+},[40] and Te^{4+},[41] respectively (see Figure 8a). The XPS spectra of compound **2** in the energy regions of Ni_{2p}, V_{2p}, and Te_{3d} give peaks at 855.3, 516.6, and 576.0 eV, attributable to Ni^{2+},[42,43] V^{5+},[40] and Te^{4+},[41] respectively (see Figure 8b). These results are consistent with the binding energy (BE) values of CuO,[39] V_2O_5,[40] $3TeO_2 \cdot Nb_2O_5$,[41] and $[Ni(C_6H_5NNC_{10}H_6O)_2]$,[42] which are 934.1 eV, 516.6, 576.1, and 855.3 eV, respectively. These results further confirm the valences of Cu, Ni, V, and Te atoms.

FT-IR Spectroscopy. The infrared spectra of compounds **1** and **2** have similar features (as shown in Figure S4). The strong bands at 967, 939, 872, and 851 cm^{-1} are due to the ν(V═O) or ν(V−O−V) vibrations. The peaks around 780, 721, and 651 cm^{-1} are ascribed to the vibrations of V−O, Te−O, Te−O−V, or Te−O−M. Bands in the 1606−1140 cm^{-1} regions are attributed to the characteristic peaks of the phen groups.

TG Analyses. The TG curve of compound **1** is shown in Figure S5a. The TG curve of **1** exhibits three steps of weight losses. The first weight loss is 4.70% from 320 to 340 °C, the second step is 9.03% from 350 to 400 °C, and the third step is 16.67% in the temperature range of 400−450 °C, all assigned to the loss of the phen groups. The whole weight loss (30.40%) is in agreement with the calculated value (29.94%).

The TG curve of compound **2** (Figure S5b) exhibits weight loss stages similar to those of compound **1**. The whole weight loss (29.50%) is in agreement with the calculated value (30.18%), corresponding to the loss of the phen groups.

Magnetic Properties of 1 and 2. The thermal variations of $\chi_m T$ and $1/\chi$ of compound **1** are displayed in Figure 6. The $\chi_m T$ versus T exhibits a value of 0.44 emu K Oe^{-1} mol^{-1} at 300 K and continuously increases on cooling to a value of 0.74 emu K Oe^{-1} mol^{-1} at 8 K. This behavior of $\chi_m T$ curve shows that there exist ferromagnetic interactions in **1**. However, the curve drops abruptly below 7 K, indicating that an antiferromagnetic interaction exists in **1** at lower temperatures. The inverse susceptibility plot as a function of temperature is linear (above 5 K), closely following the Cure−Weiss law with $C = 0.445$ emu K Oe^{-1} mol^{-1}, corresponding to about one $S = 1/2$ spin/formula unit with $g = 2.18$ for Cu(II) centers. The effective magnetic moment at 300 K, 1.91 μ_B, is in the range of experimentally observed values for Cu(II) ions. The Weiss temperature $\Theta = 8.2173$ K, indicating that there exist predominantly ferromagnetic interactions in **1**. According to the crystal structure of **1**, it can be assumed that the magnetic behavior of **1** may be due to the superexchange interactions between Cu(II) centers through the vanadium tellurites clusters.

The thermal variations of $\chi_m T$ and $1/\chi$ of compound **2** are shown in Figure 7. The $\chi_m T$ versus T exhibits a value of 1.26 emu K Oe^{-1} mol^{-1} at 300 K and slowly decreases on cooling to a value of 1.17 emu K Oe^{-1} mol^{-1} at 50 K. The curve drops abruptly below 50 K. This behavior of $\chi_m T$ curve indicates that there exist antiferromagnetic interactions in **2**. The inverse susceptibility plot as a function of temperature is linear (above 7 K), closely following the Cure−Weiss law with $C = 1.29$ emu K Oe^{-1} mol^{-1}, corresponding to about one $S = 1$ spin/formula unit with $g = 2.27$ for Ni(II) centers. The effective magnetic moment at 300 K, 3.21 μ_B, is higher than that (2.83 μ_B) of an isolated Ni^{2+} ion ($S = 1$, $g = 2.0$) with diamagnetic V^{5+} ions ($S = 0$). The Weiss temperature

(42) Yoshida, T.; Yamasaki, K. *Bull. Chem. Soc. Jpn.* **1981**, *54*, 935−936.
(43) Beyer, L.; Kimse, R.; Stach, J.; Szargan, R.; Hoyer, E. *Z. Anorg. Allg. Chem.* **1981**, *476*, 7−15.
(44) Diaz, C.; Ribas, J.; Fallah, M. S. E.; Solans, X.; Font-Bardía, M. *Inorg. Chim. Acta* **2001**, *312*, 1−6.

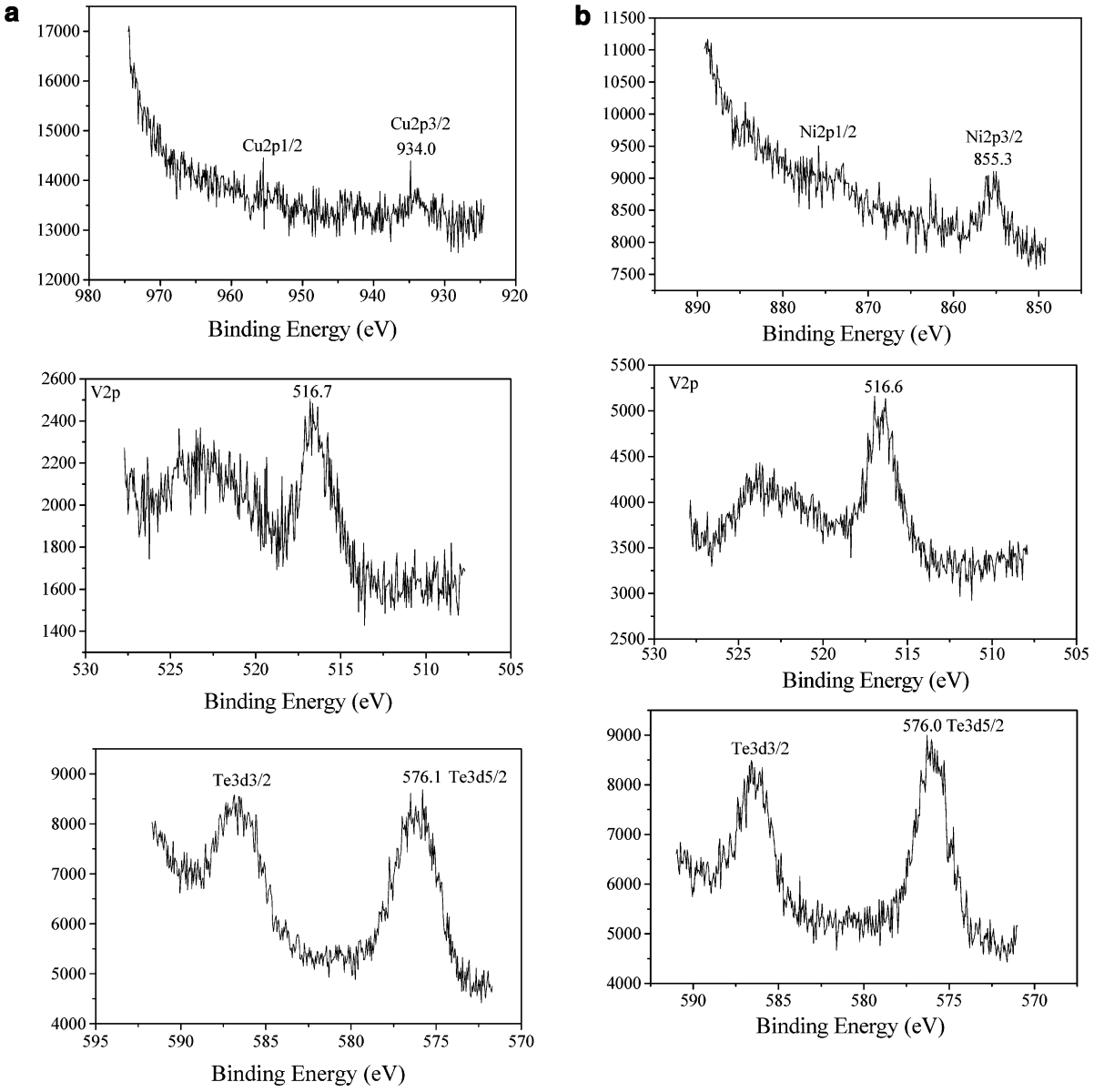

Figure 8. (a) XPS spectra of compound **1**. (b) XPS spectra of compound **2**.

$\Theta = -7.32$ K, indicating that there exist predominantly antiferromagnetic interactions in **2**. This magnetic behavior of **2** is similar to that of some reported compounds.[45]

Conclusions

In this paper, two new 2-D organic−inorganic hybrid vanadium tellurites M(phen)V_2TeO_8 (M = Cu (**1**) and Ni (**2**)) have been reported. Compounds **1** and **2** contain novel $[V_2TeO_8]_\infty$ double-chain-like ribbons bridged by metal−organic complex moieties. The successful isolation of compounds **1** and **2** not only confirms that novel organic−inorganic hybrid vanadium tellurites can be obtained by the introduction of different metal−organic complex moieties but also provides an interesting matrix for the preparation of novel organic−inorganic hybrid tellurium-containing materials. Further research in this subclass may concentrate on the replacement of copper and nickel with other metals and phen with other organic ligands and the exploration of their attractive properties.

Acknowledgment. This work was financially supported by the National Science Foundation of China (Grant 20171010).

Supporting Information Available: X-ray crystallographic files in CIF format for compounds **1** and **2**, an OPTEP for **2**, a view of the organic−inorganic 2-D network of **2**, the packing arrangement of compound **2**, and IR spectra and TG curves of compounds **1** and **2**. This material is available free of charge via the Internet at http://pubs.acs.org.

IC034272P

(45) Liu, C.-M.; Gao, S.; Hu, H.-M.; Jin, X. L.; Kou, H.-Z. *J. Chem. Soc., Dalton Trans.* **2002**, 598−601.